Chinese Science Bulletin 2004 Vol. 49 No. 22 2405—2414

Effects of soil amplification ratio and multiple wave interference for ground motion due to earthquake

ZHAO Zhixin[1], XU Jiren[1] & Ryuji Kubota[2]

1. Institute of Geology, Chinese Academy of Geological Sciences, Beijing 100037, China;
2. Kawasaki Geological Engineering Co., Ltd., 2-11-15 Mita Minato-ku, Tokyo 108-8337, Japan

Correspondence should be addressed to Zhao Zhixin (e-mail: zhaozhixin@ccsd.org.cn)

Abstract **Influences on the ground motion simulations by soil amplification effects and multiple seismic wave interferences in the heterogeneous medium are investigated. Detailed velocity structure obtained from the microtremor array survey is adopted in the ground motion simulation. Analyses for amplification ratios of core samples of ten drill holes with 40 m deep in the sedimentary layers show that the soil amplification ratio influences nonlinearly the seismic ground motion. Based on the above analysis results, the ground motion in the heavily damaged zone in the Japanese Kobe earthquake of 1995 is simulated in a digital SH seismic wave model by using the pseudospectral method with the staggered grid RFFT differentiation (SGRFFTD). The simulated results suggest that the heterogeneous velocity structure results in a complicated distribution of the maximum amplitudes of acceleration waveforms with multiple peaks at the surface. Spatial distribution of the maximum amplitudes coincides well with that of collapse ratios of buildings in Kobe. The dual peaks of the collapse ratios away from the earthquake fault coincide well with the double peak amplitudes of simulated seismic acceleration waves also. The cause for the first peak amplitude of the ground motion is attributable to the interference of the secondary surface wave from the bedrock propagating horizontally along the surface sedimentary layer and the body wave from the basin bottom according to analyses of wave snapshots propagating in inhomogeneous structure of the Osaka group layers. The second peak amplitude of the ground motion may be attributive to the interference of the secondary surface wave from the tunneling waves in the shallow sediments and the body wave. It is important for the study on complicated distributions of earthquake damages to investigate influences on the ground motion by soil amplification effects and multiple seismic wave interferences due to the structure. Explorations of the structure to the bedrock are necessary for the urban mitigation disaster. Seismic wave simulations are valid for aseismatic study.**

Keywords: soil amplification ratio, wave multiple interference, ground motion acceleration, earthquake damage, numerical simulation.

DOI: 10.1360/04wd0002

Study on seismic disaster is quite important for protecting the lives and properties of the people[1]. Many prevention disaster projects in civil constructions, etc. require quite accurate and reliable ground motion parameters. It has great social and economic effects to analyze the damage mechanisms and destructive processing of buildings by means of investigations of quantitative ground motions. Numerical simulations of seismic ground motion have been increasingly developed with the popularization of computer application[2—4]. Physical factors clarifying the natures of ground motion can be quantitatively investigated by digital simulation of seismic wave propagating in the inhomogeneous medium[5,6].

The causes for destroyed buildings are perhaps related to both buildings and seismic ground motions. The ground motion is closely related to geological structure. For example, buildings nearby the active fault are easy destroyed as the earthquake occurs along the faults usually. The building damage is also related to the base structure of buildings that can be destroyed by the secondary effects of earthquake, e.g. liquefaction of soil and landslip etc.[7]. The damaged zone due to the base structure destructions is smaller than that due to the geological structure influences generally. Disaster causes due to both structures mentioned above can be directly understandable usually. Some complicated distributions of heavily damaged zones, however, are hardly understandable based on merely geological structure distribution. The buildings are destroyed by the ground oscillations during earthquake occurrence. The destroyed causes of buildings are quite complicated indeed, it might be related to dynamic and kinematic characteristics of the medium[8,9] besides underground geological structure. The damage causative mechanism is discussed in the following.

A building having quality m at the surface is accelerated by an acceleration a on the base structure from the ground motion during earthquake occurring. It means that a force f acts on the building (or building base). The magnitude is calculated as follows:

$$f = ma. \quad (1)$$

The acceleration force coming from the ground motion collapses buildings at the surface. Earthquake disasters and the ground motions attenuate generally with distance away from earthquake fault[10,11]. Many complicated anomalous distributions of earthquake damages, however, have ever been reported after some earthquakes. The damages do not simply attenuate with the distance away from the fault in that case. Damaged zones and seismic intensities reveal complicated distributions by influences from geological structure[12]. For example, the anomalous seismic intensity occurred in Yutian region, Hebei Province, China in the Tangshan M7.8 earthquake in 1976. The intensity in Yutian was lower than that in the vicinities. The low intensity was explained by the site effect[13]. A notable heavily damaged zone due to the 1995 Hyogo-ken Nanbu, Japan sharp earthquake like a belt appeared away from the aftershock zone that is taken as the earthquake

fault usually (Fig. 1). The aftershock zone near N53°E, extending along the root of the Rokko Mountain, coincides well with regions of the active faults. The damaged belt approaches to the Osaka Bay being 1 or 2 km away from the aftershock zone on average. The spatial distribution discrepancy between the heavily damaged belt zone and the aftershock zone (or the earthquake fault) has been widely discussed. The spatial distribution of collapse ratios of buildings has a complicated character even in the narrow heavily damaged belt zone. Few papers deal with the problem. The complicated distribution property of collapse ratios of buildings with multiple spatial peaks in the heavily damaged zone is further investigated in the present analysis. The destructive force of building damages comes from the ground acceleration as shown in eq. (1). The analyses for spatial distributions of the ground motion and the physical factors impacting on the ground motion acceleration are beneficial to investigating the cause of the complicated distribution of collapse ratios.

The distributions of the ground motion are probably related to characteristics of geological structure beneath the surface. To investigate the cause of abnormal distribution of collapse ratios of buildings in Kobe earthquake (Fig. 1) in detail, a new 2-D detailed seismic wave velocity structure has been surveyed by a micro tremor array and the results are used in the analysis of this paper. The investigations of amplification effects for core samples of the ten drill holes of 40 m deep at the sediments in the Osaka group layers were carried out in detail. Based on the above results of geological effect, the cause of collapse ratios of buildings with multiple peaks is investigated by seismic simulations in heterogeneous medium using the pseudo- spectral method with a staggered grid RFFT differentiation[14].

1 Distribution of collapse ratios of buildings with multiple peaks

The M7.2 earthquake having multi-source ruptures occurred in Hyogo-ken Nanbu (Kobe, 35.03°E, 34.58°N) in 1995[15]. The black bars A, B and C along about NE direction represent the three sub-faults of the multiple source rupture processes for the main shock as shown in Fig. 1[10,16]. The sub-faults are all strike-slip type events, and their parameters are shown in the caption of Fig. 1. Starting crack points of the three sub-faults in the theory on the crack propagating with prescribed velocity are 5, 15 and 8 km deep, respectively. Seismic damages were investigated in detail in Kobe City after the earthquake. Two notable characteristics about damage distribution are reported. Firstly, the heavy damage distributes unilaterally to the southeast of the source fault like a narrow belt, and away from the aftershock zone (earthquake fault) as shown in Fig. 1. The belt aftershock zone extending along the root of the Rokko Mountain coincides well with the region of active faults. To investigate the characteristics of the collapse ratios of buildings many geological and geophysical surveys have been carried out. Any active or buried fault has not been found beneath the heavily damaged belt zone yet (Fig. 1)[10]. The abnormal damage distribution is perhaps related to other factors of the ground motion[17,18]. Secondly, the collapse ratios of buildings in the heavily damaged belt zone as mentioned above did not

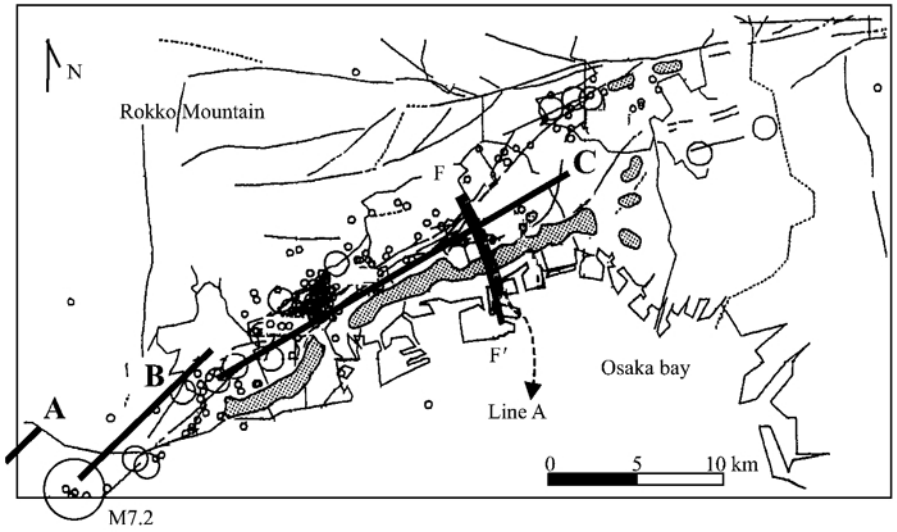

Fig. 1. Aftershock zone and heavily damaged zones in Kobe City for the 1995 Hyogo-ken Nanbu M7.2 earthquake, Japan (35.03°E, 34.58°N) (modified after the Department of Earthquake and Volcano, Japan Meteorological Agency (JMA)). Big open circle: main shock; hatched area: JMA intensity 7 zones; solid line: active faults; open circles: aftershocks. Line FF′: survey line of velocity structure by the micro tremor nets. Black dash line A: survey lines of collapse ratios of buildings in the Higashinata (NG) ward, Kobe City. Black bars A, B and C: three sub-faults of the multiple source rupture processes of main shock[16]. Strike direction and dip angle of sub-fault plane A: (N45°E, 82°); B: (N53°E, 90°); C: (N233°E, 85°). Kanan University is located near the cross between fault C and line FF′.

monotonically attenuate with the distance away from the earthquake fault. The collapse ratios varied severely with multiple peaks and troughs in the strike perpendicular to the earthquake fault[19]. In the present analysis the cause for inhomogeneous distribution characteristics of the collapse ratios with two peaks along the survey line shown by dash line A in Fig. 1 are investigated in detail.

The zones with seismic intensity (Japanese Meteorological Agency (JMA) scale) 6, or greater like a narrow belt about 20 km long and 2.0 km wide and heavy damages only distributed to the southeast of the source fault (the aftershock zone), approaching to the coast of the Osaka Bay as shown in Fig. 1. The heavily damaged zones never occurred northwest of the source fault. The areas of the intensity being equal to or greater than 7, corresponding to collapse ratios of wooden buildings being equal to or greater than 30%, shown as hatched area in Fig. 1, distribute heterogeneously in the heavily damaged zone. The black dash line A, almost perpendicular to the aftershock zone, in Fig. 1, represents the detailed investigation lines of collapse ratios of buildings in the Higashinada ward, Kobe in the heavily damaged belt zone. The investigation line A crosses the heavily damaged belt zone. The collapse ratios of buildings were investigated in sedimentary region along line A from the earthquake fault (near the original point of abscissa axis in Fig. 2) to the coast of the Osaka Bay. Fig. 2 shows the detailed results of the collapse ratios of buildings investigated along the dash line A about 3.5 km long[20]. These investigated results are based on both wooden houses and steel concrete buildings. The collapse ratios did not monotonically attenuate with distance away from the earthquake fault along dash line A. The intensity varied between 6 and over 7. Two peaks of collapse ratios

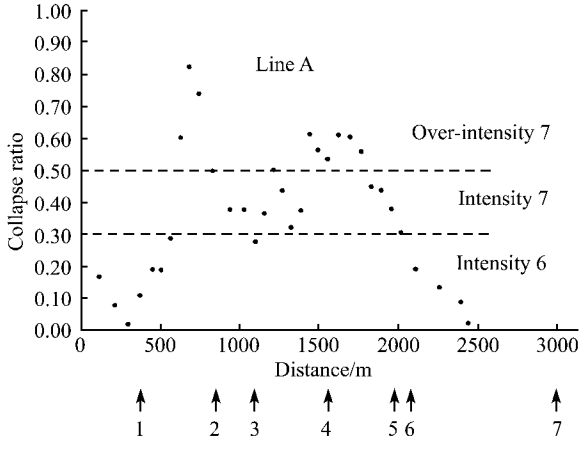

Fig. 2. Collapse ratios of the buildings along dash line A in Fig. 1 in which original point is near the source sub-fault C, another end of distance axis is near the coast of Osaka Bay[20]. Arrow marks under the distance axis represent the locations: ↑1, Hankyu Kobe railway; ↑2, JR Kobe railway; ↑3, Gokudo No.2 Highway; ↑4, Kawai Park; ↑5, Hanshin railway; ↑6, Gokudo No.34 highway; ↑7, coastline.

clearly appear (Fig. 2). One of the peak collapse ratios is greater than 80% near the JR Kobe railway (place ↑2) where the intensity is over 7. Another peak of collapse ratios is greater than 60% in the Kawaii Park (↑4) where the intensity is greater than 7. Collapse ratios around the highway Gokudo No.2 (↑3) are about 40%, less than that at either vicinity. It is a trough in the value of collapse ratios along line A between the above two peaks of seismic intensity over 7. The collapse ratios along dash line A gradually decrease from the Kawaii Park (↑4) toward the sea beach in the direction of southeast.

In order to understand the causative mechanisms of collapse ratios with multiple peaks, influences on the ground motion by seismic velocity structure and soil amplification are investigated in the following sections employing digital simulation method. The multiple peak ground motion and the corresponding causative mechanism of the damages are studied by employing spatial distribution characteristics of seismic waveform amplitudes and snap shots of seismic wave propagation obtained from digital simulation.

2 Velocity structure and soil amplification ratios

Inhomogeneous geological structure, properties of rock and soil layer influence strongly propagation of seismic wave. The granite bedrock emerges in the Rokko Mountain northwest of the aftershock zone (Fig. 1). The belt aftershock zone extends along the root of the Rokko Mountain near the NE direction. Sedimentary layers, the Osaka group layers overlaying the bedrock thicken gradually approaching the coast of the Osaka Bay of Kobe City. The heavily damaged zones distribute nearly in the Osaka group layers formed from three sedimentary layers southeast of the earthquake fault as shown in Fig. 1.

A 2-D exploration of seismic velocity structure was carried out in detail using the microtremor array survey along the solid line FF′ (Fig. 1) in order to analyze the cause of distributive characteristics of the collapse ratios of buildings with multiple peaks. According to principle of the microtremor method, velocity structures beneath the observatory and its surroundings can be inversed by analyzing microtremor waveforms at the ground[21]. The microtremor waveforms are observed with an array survey that can record microtremor signals within a defined frequency domain at the surface. Line FF′ is almost superposed on investigation line A of the collapse ratios, which is perpendicular to the strike of the earthquake fault. F side is near the Rokko Mountain, F′ side is close to the coast of Osaka Bay. The 2-D velocity structure of S-wave in Fig. 3 is modeled after the survey data of the microtremor array. The fault thrusting from the NWW to SEE direction obtained from the reflection survey results outcrops near Kanan University marked as the downward arrow in Fig. 3[10]. The Kanan University is about 5 km away from F side, near the cross between the Fault C and

Line FF′ in Fig. 1. The bedrock of granite (Ⅳ) emerges on the left side of Kanan University (the Rokko Mountain region between F and the arrow (Fig. 3)). The university is next to the boundary between bedrock and the Osaka group layers at the surface. The Osaka group layers are modeled as three sedimentary layers, the upper (Ⅰ), middle (Ⅱ) and lower (Ⅲ) overlie on the bedrock (Ⅳ) in the right zone of profile (Fig. 3) (between the arrow and F′). Wave velocities and densities of the four regions are shown in Fig. 3, respectively. Any fault has not been found beneath the locations of peak collapse rations (Fig. 2) based on the above analyses of microtremor data.

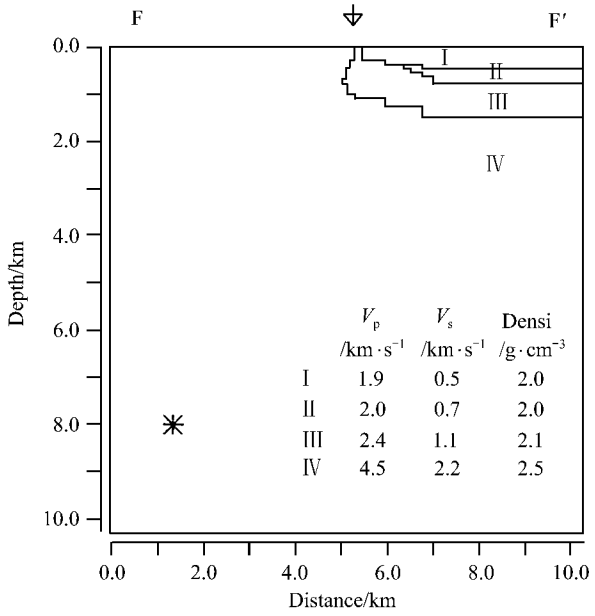

Fig. 3. Velocity structure in the FF′ profile in Fig. 1 modeled after results surveyed by the micro tremor technique. Layers Ⅰ, Ⅱ and Ⅲ are the upper, middle and lower portions of the Osaka group layers, VI is the granitic bedrock layer. V_P, V_S and Densi are P-, S-wave velocities and density of each layer. The downward arrow marks the Kanan University. The asterisk represents the source in the simulation by the pseudospectral method.

Amplification effects of shallow sedimentary layers probably vary with the sites at the surface. To investigate the cause of the collapse ratios of buildings with multiple peaks in Fig. 2, the influences on ground motions from seismological dynamic characteristics of the medium structure beneath the Osaka group layers along FF′ line in Fig. 1 were analyzed in the present analysis. The investigations on boreholes of 40 m deep were ever carried out at ten sites along line FF′ in the heavily damaged zone over the Osaka group layers. Soil core samples of 40 m deep were gathered from the drilled holes too. The influences upon the amplitudes of seismic waveforms by the shallow sedimentary soil layer were analyzed employing the soil core samples with 40 m deep at the ten sites along FF′ line. The rate about the maximum amplitude of output response waveform at the surface of 40 m deep drill core to unit impulse input at the bottom of the borehole core is taken as the amplification effect for seismic wave passing through the soil layer at each site by analyzing characteristics of the response waveform. Amplification effects of soil core samples of ten drill holes with 40 m deep along line FF′ are shown in Fig. 4. The top figure shows the response waveforms on the surface of the unit pulses input at bottoms for the ten sedimentary drill core samples[22], respectively. The asterisks in the middle diagram show the corresponding amplification ratios of output waveforms to input unit pulses for seismic waves passing through drill soil cores of the ten bore holes. The bottom diagram shows the structure profile in Fig. 3 in order to understand the relationship between amplification functions and soil layers at sites. Fig. 4 depicts that the amplification effects of shallow sediments beneath the Osaka group layers are quite different among the sites. The maximum value of the amplification ratios is about four times greater than the minimum one. The maximum rate is 3.123, displaying soil amplified effect. The minimum is 0.864, however, less than 1.0 displaying reduced effect. Such ratios in Fig. 4 display the nonlinear property of amplification effect of shallow sediments in the Osaka group layers in the heavily damaged zone. The amplification ratios to the unit pulse for the sediments decrease gradually from Kanan University (down arrow in Fig. 4) to the coast of the Osaka Bay

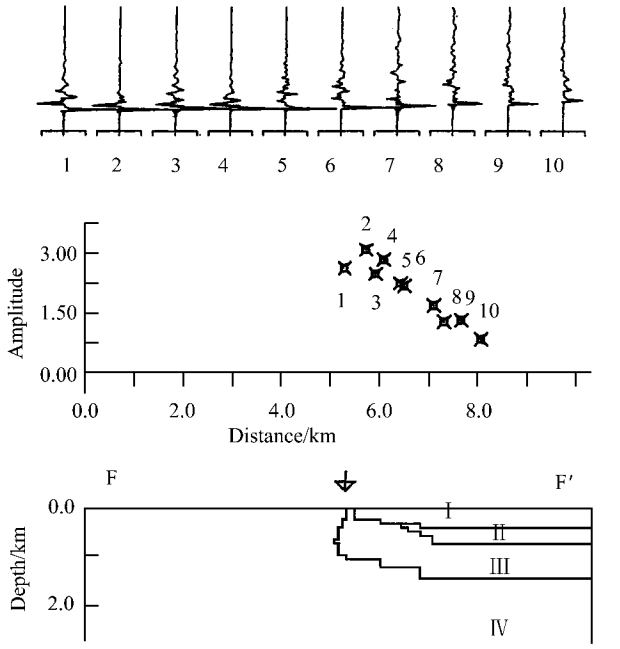

Fig.4. Amplification ratios for the soft soil core samples of 40 m deep drill holes at the ten sites along line FF′ in Fig. 1. Bottom diagram: structure profile in Fig. 3. Down arrow for the Kanan University. Middle figure: amplification ratios of the soft soil for 10 drill cores. The ordinate for the amplification ratio of seismic wave, the abscissa for the locations of the bore holes. Top figure: 10 output response waveforms of the unit pulses input from the bottom for the drill core samples.

(near F′ side in Fig. 1). The average value of the amplification ratios on the right four sites (7th—10th) near the coast of Osaka Bay is about one half of that on the left six sites (1st—6th) near Kanan University.

3 Simulation of ground motion acceleration and collapse ratios of buildings

The distribution of ground motion and wave propagation process in the profile FF′ in Fig. 1 was simulated to investigate the relationship between amplitude distribution of ground motion and seismic velocity structure. The inhomogeneous geological structures might influence distributions of the ground motion resulting in abnormal characteristics of building damages. The seismic wave fields are usually computed by resolving wave equation with discrete numerical differentiation method[23] as the lateral heterogeneity of medium structure can not be neglected. The earthquake damages are generally related to the frequency, amplitude and lasting time of seismic wave[24]. Source frequency and seismic wave time length of calculation should be rationally selected as simulating the cause of building damage distribution with the two peaks.

(ⅰ) Simulation of acceleration waveform. In order to analyze the cause of earthquake damages, the influences on the distribution of collapse ratios of buildings with multiple peaks by velocity structure in Fig. 3 and sediment amplification rates in Fig. 4 were investigated by employing the ground motion simulation with the pseudospectral method. This computerized modeling method has been widely employed in seismic simulation because of its high speed, high resolution and efficiency in use of the computer memory[25—27]. The SGRFFTD operator, a speedy, highly accurate and stable technique, was used in the simulation[3,28,29]. The simulation with a 2-D SH problem model was used in the ground motion calculation over the profile in Fig. 3 to analyze the cause of distribution with the two peak collapse ratios. The SH seismic wave equation can be expressed as follows in the staggered grid case.

$$\rho_{n,m}\dot{v}_{yn,m} = \partial\tau_{xyn+1/2,m}/\partial x + \partial\tau_{yzn,m+1/2}/\partial z + f_y. \quad (2)$$

In eq. (2), τ is the stress, $\tau_{xy\,n+1/2,m}$ means that stress τ is sampled and calculated at the n+1/2, m. n+1/2 is at the middle between the nth and (n+1)th grid. ρ is the density at the point x, $\dot{v}$ is the first order differentiation of ground motion velocity to time, f is the density of body force. Lame constants and ρ are defined at the center of grid.

The structure model in Fig. 3 was sampled with 256 × 256 grids at 40 m spacing in both horizontal (as x) and depth (z) directions in the discrete numerical simulation. The limiting frequency in the simulation can be considered as 6.25 Hz in such a case. Time interval was taken as 0.008 s. The asterisk in Fig. 3 represents the line source. The line source force perpendicular to the profile was taken as a Gaussian shape spatial function with a Ricker wavelet source time function having a peak frequency of 3.5 Hz. The peak period in source function was selected referring to the intrinsic periods of relative buildings. The intrinsic periods for wooden house and buildings lower than 50 m nearly are in the period between 0.1 and 1.0 s. The test results show that intrinsic periods of civilian engineering and mansions are in period between 0.2 and 0.4 s in Shanghai, China[30]. Three factors of seismic wave vibration, amplitude, frequency and lasting time usually character strong ground motion. The source peak frequency of 3.5 Hz employed in the simulation approaches the natural frequency of the buildings lower than 50 m. Therefore, it is valid that the simulation results are used to clarify the relationship between the collapse ratios and maximum amplitudes of acceleration waveforms. The seismic waveforms with the duration of 18 s were simulated. The absorbing boundary condition[31] was applied to the lateral and bottom edges of the spatial grids. The free-surface condition was approximated by including 256-point zero shear velocity above the upper surface of the model in vertical derivatives of stress. The symmetric differentiation method[32] was applied to vertical differentiation of displacement to stabilize the derivatives in the surface nodes.

(ⅱ) Comparisons for collapse ratios of buildings and ground motions. Fig. 5 shows the simulated ground motion results over the profile FF′ of velocity structure in Fig. 3. For convenience of comparison, the bottom, middle and top diagrams in Fig. 5 show the structure, simulated seismic waveforms at the surface and the comparison of maximum amplitudes of simulated waveforms in the duration of 18 s to collapse ratios with the same abscissa scale, respectively. In the bottom diagram the node (or node line) of the thrust fault plane near Kanan University is located at about the 128th grid at the surface. In the middle diagram simulated seismic waveforms at the bedrock sites to the left of Kanan University are simple and close to each other because the waves from the source arrived directly at the sites only passing through the united homogenous structure of bedrock (Ⅳ region). Acceleration seismic waveforms at the sites in the Osaka group sedimentary layers (on right side) are different from each other. The differences are probably related to the complicated wave properties and the various amplification effects of the multilayered medium where the waves pass. Several late seismic phases, including the surface waves, transformed wave phases at the free surface and intersurfaces complicate evidently the waveform in seismograms at the sites on the Osaka group layers, and last longer time for vibrations in the right sedimentary region compared with those on the left bedrock side (F). The great waveform amplitudes occur near the JR Kobe railway (place ↑2) and the Kawaii Park (↑4). The amplitudes around the

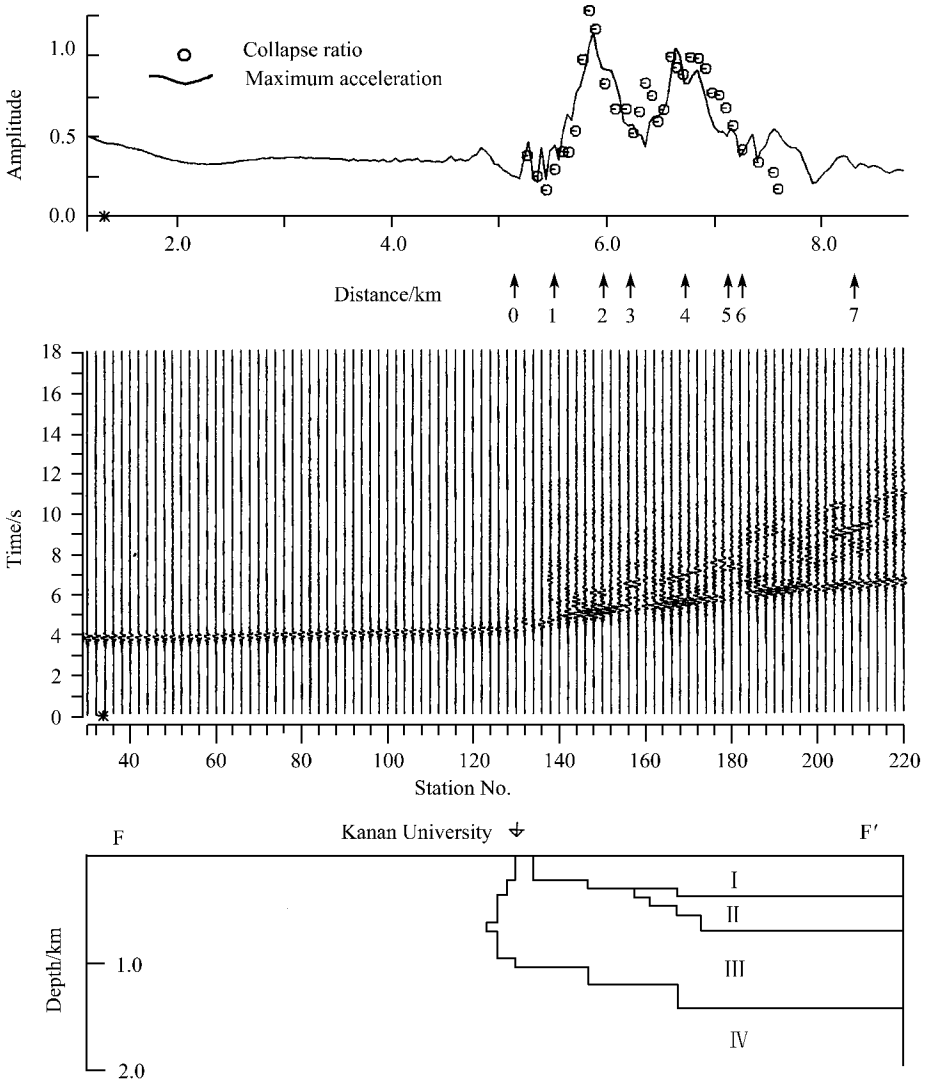

Fig. 5. Comparison between the structure, collapse ratios of buildings due to the 1995 Hyogo-ken Nanbu earthquake and the maximum amplitudes of simulated seismic waveforms along dash Line A in Fig.1 with the same distance scale. Bottom diagram: structure of vertical section FF′ in Fig. 3. Middle diagram: simulated acceleration waveforms at the sites along FF′ line. Asterisk: the source in Fig. 3. Top figure: comparison between collapse ratios of buildings (open circles) and the maximum amplitudes (solid line) of acceleration waveforms corresponding to those in the middle figure corrected by the soil amplification effects underneath the sites obtained from those in Fig. 4. The maximum amplitudes of waves and the collapse ratios are standardized as arbitrary unit dimension. Arrows from ↑1 to ↑7 under the distance abscissa represent the same locations as those along Line A in Fig. 2. ↑0: for Kanan University. Original point is at earthquake sub-fault C in Fig. 1.

highway Gokudo No.2 (↑3) are relatively little. The amplitudes of the primary arrival phases of waves in the sites near the thrust fault node plane (↑0) are less than those to either side.

The soil amplification ratios are closely related to the components, structure and the pore volume in the medium of borehole cores. Therefore, the impacts on the amplitudes of acceleration seismic waveforms by the soil amplification ratios of borehole cores at ten sites in Fig. 4 are different from each other. Furthermore, seismic waveform amplitudes are influenced by multiple actions of the wave fields except nonlinear soil amplification ratio. For the foundational geological investigations of building engineering, the supporting structure layer of buildings is generally less than 30—40 m deep. The soil amplification ratios below the supporting structure layer are much more stable and homogeneous than those above the sporting layer usually. The soil amplification ratios of borehole cores of 40 m deep in Fig. 4 were taken as the site factor used in calculations of the acceleration waveform. The corresponding amplification ratio at each site in the Osaka group layers along FF′ was calculated by interpolation technique from the ratios at ten sites in Fig. 4. The collapse ratios of buildings (open circles) are compared with

the maximum amplitudes of acceleration waveforms in the middle diagram multiplied by the soil amplification ratios as shown in the top diagram in Fig. 5 (solid line). In the top diagram in Fig. 5 the secondly peak amplitudes of both collapse ratios of buildings and ground accelerations are standardized as the same amplitude (arbitrary unit) for the comparison convenience. The maximum amplitudes of waveforms at the bedrock sites on the left side to Kanan University (arrow ↑0) vary evenly and smoothly. The amplitudes of waveforms at the Osaka group layers, on the right side of figure, however, vary intensely with multiple peaks and troughs. The first peak of the amplitudes appears on the sedimentary side near site ↑2 near 4.8 s (middle diagram in Fig. 5). The second peak amplitude appears on the sedimentary side near site ↑4 near 5.6 s. The distribution of amplitudes of simulated acceleration waveforms fits well that of the collapse ratios of buildings in the time and space as a whole. Two peak waveform amplitudes coincide well with those of the collapse ratios also. Such a spatially coincident distribution implies that the complicated distribution of collapse ratios is probably an attribution for the seismic motion influenced by the underground structure.

Furthermore, in Fig. 4, the average value of the amplification ratios of 40 m soil core of shallow sediments in the right four sites (from the 7th to 10th) greater than 6.8 km away from the original point near the coast of Osaka bay is about one half of that in the left six sites (from the 1st to 6th) near Kanan University. The collapse rations of buildings in the right zone near the coast of Osaka bay in Fig. 5 are correspondingly less than those in the left zone approaching Kanan University on an average. It implicates that soil amplification ratios for the shallow layer impact deeply the collapse rations of buildings in Kobe City. This result is one of the discussing topics in the present analysis. Some particular variations of the collapse ratios may not well coincide with the soil amplification function. This is because distribution of the collapse ratios may be influenced by wave transformations and interferences in inhomogeneous medium except the soil amplification effects. Specially, the peak and trough collapse rations are deeply influenced by mutual actions among the original and various secondary waves[19,33]. This is another topic and discussed further in the following. Some recent studies show that there is a good correlation between the collapsing rate and peak ground velocity, rather than the peak ground acceleration. The result is also consistent with that simulated in a single source frequency in the present analysis.

4 Discussion on the cause of ground motion with multiple peaks

The distribution of ground acceleration motions depended on the seismic velocity structure and soil amplification effect was discussed for the heavily damaged zone in Kobe City. The results show that the distribution of the collapse ratios of buildings along line A coincides well with that of the maximum amplitudes of acceleration waveforms. Peaks of waveform amplitudes are almost superposed on those of the collapse ratios of buildings. The coincident spatial distributions suggest that the accurate analyses for soil amplification effect, geological and velocity structures are beneficial to clarifying the cause of complicated distribution of building collapse. Therefore, analyses of nonlinear amplification effect of the soft soil and geological structure are important for aseismatic study[10]. The Osaka group layers approaching the sea beach are thicker than those near Kanan University as shown in Fig. 4. The soil amplification ratio of the former, however, is less than one third of the latter. The heavily damaged belt did not appear in the thick sediments as shown in Fig. 5. The results show that the relationship between the collapse ratios and the soil thickness may not be a direct ratio in the case.

The wave interference can be formed by the direct body wave from the basin bottom and the secondary surface wave in and around the basin region[19]. The interference could further result in peaks of the ground motion and heavy seismic damages[3,19]. Fig. 6 illustrates the interference occurrences in the wave propagation in the structure model in Fig. 3 by means of simulated wave snap shots. The wave propagated with a spherical wavefront in region Ⅳ before 4.0 s. In snap shot at 4.0 s, the wave with spherical wavefront in region Ⅳ refracted into region Ⅲ at the bottom boundary of region Ⅲ and transformed as a plane wavefront. The wave refracted upward into regions Ⅱ and Ⅰ again at shots 4.8 and 5.6 s. In left granite bedrock region Ⅵ, the wave arriving in the free surface reflected in 4.0 s, while a rightward wave passed through the thrust fault plane and propagated along the sedimentary layers Ⅰ, Ⅱ and Ⅲ. The waves propagating along the surface layer are taken as the secondary surface waves[19]. The interferences occurred as the upward body wave met the rightward secondary surface wave propagating along the surface from region Ⅳ to region Ⅰ in 4.8 and 5.6 s (seeing the shots in Fig. 6), respectively. Such interferences in the structure in Fig. 3 can result in the peak ground motions that are causes of heavy seismic damages, high collapse ratios as shown in Fig. 5 and the inhomogeneous distributions of damages in Fig. 1. The interferences of the ground acceleration waves are away from the boundary between the outcropping bedrock and the Osaka group layers in Figs. 6, and so do that of the collapse rations. Distance between the interference peak and the fault node is related to the velocity differences between rock region Ⅳ and the multilayered Osaka group layers. More wave phases appearing at the snap shot in 5.6 s might result in multiple complicated ground motions and heavy damages.

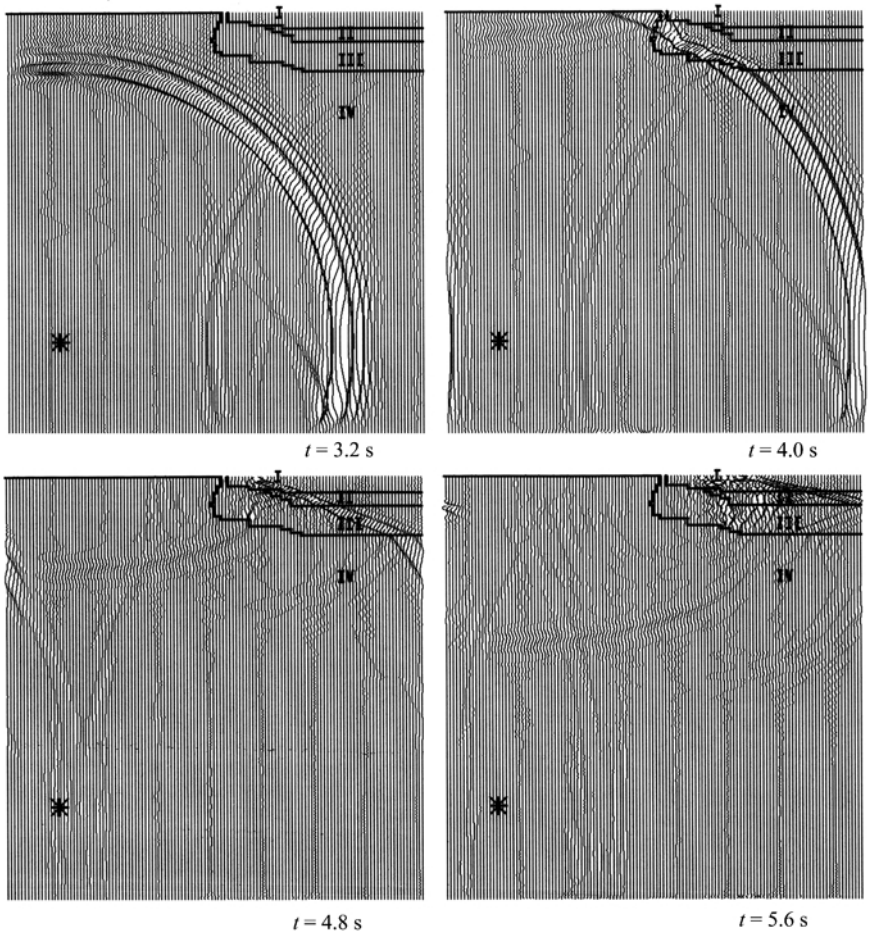

Fig. 6. Snap shots of seismic wave simulated in the profile FF′ of heterogeneous velocity structure in Fig. 3. Thrust fault is about 5 km away from the left end, corresponding to about 128 grads in Fig. 3. Regions Ⅰ, Ⅱ, Ⅲ and Ⅳ have the same medium parameters as those in Fig. 3.

The illustration suggests that the peak distribution of the collapse ratios along survey lines A is attributable to peak amplitudes of the ground acceleration motions based on analysis of the above coincident distributions.

In order to clearly show the interference process, Fig. 7 illustrates only the wave propagation by snap shots in shallow parts in Fig. 6. The secondary surface wave started to enter in to region Ⅰ crossing the boundary between regions Ⅳ and Ⅰ in the snap shot in 4.0 s, the body wave did not arrive in region Ⅰ, propagating still in region Ⅲ. In the snap shot in 4.8 s, the body wave with the plane wavefront occurring at the bottom boundary of region Ⅲ refracted upward into regions Ⅱ and Ⅰ, three plane waves propagated up-rightward with different apparent velocities in layers Ⅰ, Ⅱ, Ⅲ. Normal directions of the three plane wavefronts were somewhat different from each other. The interference occurring as the upward body wave met the secondary surface wave in layer Ⅰ in site about 20 grids away from the boundary between the outcropping bedrock and the sedimentary layer (about 150 grids away from the original point). The location and time bringing forth the first wave interference in Fig. 7 coincide well with those bringing about the first peak ground acceleration and first peak collapse ratio in Fig. 5. At the snap shot in 5.6 s, wave propagations become more complicated. The surface waves (or tunneling waves) grow well in the three sedimentary zones of the Osaka group layers. The surface waves, however, attenuated rapidly outside the bottom of layer Ⅲ in region Ⅳ. The periods of growing surface waves are greater than those of refracted body waves with plane wavefronts. The surface wave with low frequency met the upward body wave at the surface at the shot of 5.6 s, and the second interference occurred in site about 20 grids away from the first interference location at the shot of 4.8 s (about 170 grids away the original point). The location and time bringing forth the second wave interference in Fig. 7 are coincident with those bringing forth the secondly peak ground acceleration and secondly peak collapse ratio in Fig. 5 also. At the shot of 5.6 s, the wavefront of low frequency surface wave behind the rightward body wave slantingly faced upward

in layer Ⅰ. The wavefront of surface wave (or tunneling wave) vertically faced ahead in layer Ⅱ, and slantingly faced downward in layer Ⅲ. The causes forming the three surface (tunneling) waves linking to each other are not clear yet. It seems that the surface wave reflecting at the free surface in the left bedrock zone transmits into the basin from the basin lateral bottom according to analyses of snap shots in Fig. 7. The strong secondary wave phases (the surface waves) can be clearly seen as wave fields transmit into the medium with low velocity from the medium with high velocity at the snap shots. Correspondingly, the reflection phases can hardly be seen. It may imply that the transmission energy or coefficient is strong and can result in heavy damages at surface in the above case. It is also very important in the aseismic study of basin[29]. The above analyses suggest that the secondary multi-phases probably result in wave multiple interferences in various places in the multi-layers medium depending on the regional geological structure. The multiple peak ground motions due to the interferences can result in complicatedly inhomogeneous distribution of heavy earthquake damages with peak collapse ratios of buildings as shown in Figs. 2 and 5.

The present analysis shows that the distribution of collapse ratios of buildings is closely related to the detailed deep structure in Fig. 3 and the soil amplification effects of shallow layer. Therefore, the detailed geological information of the basement complex is important for analyzing the cause of the collapse ratios, prediction of strong ground motion, as well as for the aseismite projects in the urban area. In another respect, the present analyses imply that the simulation of seismic wave is available for the study of the ground motion prediction.

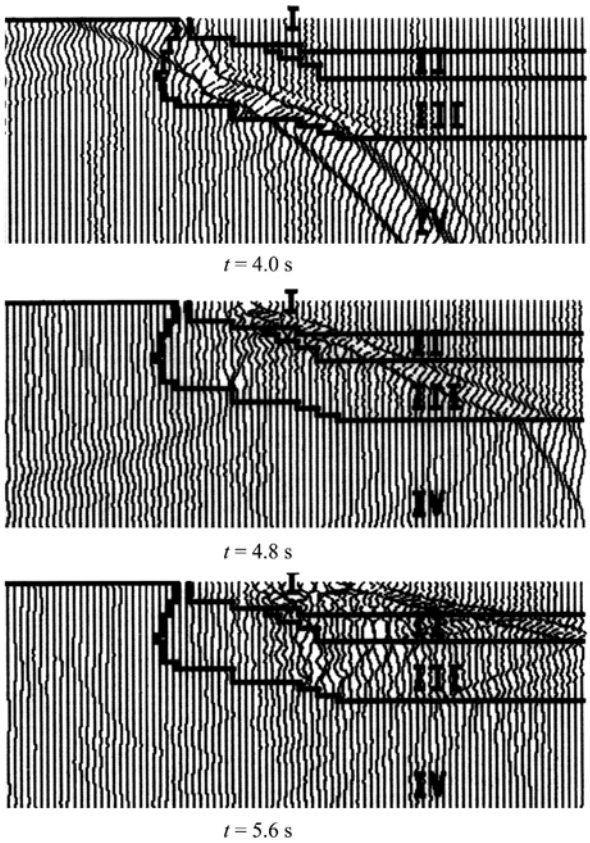

Fig. 7. Snap shots of wave propagation in the shallow parts of structure model in Fig. 6. The display manners are the same as that in Fig. 6.

5 Conclusion

The effects for soil amplification and wave multiple interferences in the seismic ground motion simulations were investigated in the present analysis. The results are summarized as follows:

(ⅰ) The amplification effects in the soft soil nonlinearly influence the ground motion and collapse ratios of buildings in the Osaka group layers. It is important for seismic wave study to analyze the soil amplification effect.

(ⅱ) The seismic wave simulations show that the ground acceleration motions with multiple peaks are attributable to the multiple interferences closely related to the geological and seismic velocity structure. The distributions of maximum amplitudes of ground acceleration waveforms with multiple peaks coincide well with those of the multiple peak collapse ratios in Kobe City. The results suggest that the complicated distribution of the collapse ratios of buildings in heavily damaged belt zone is attributable to the multiple seismic wave interferences related to the underground structure and the soil amplification ratios.

(ⅲ) The geological information of basement complex is important for study of the ground motion. Furthermore, a detailed survey of the foundation structure to the bedrock is beneficial to the mitigation and prevention of disasters.

(ⅳ) The digital simulation technique is available for study on collapse ratios of buildings and aseismic study.

Acknowledgements This work was supported by the 973 Project of the Ministry of Science and Technology of China (Grant No. 2003CB716505) and the National Natural Science Foundation of China (Grant No. 40399141).

References

1. Frankel, A., Mapping seismic hazard in the central and eastern United States, Seism. Res. Let., 1995, 66: 8—21.
2. Graves, R. W., Three dimensional finite difference modeling of the San Andreas fault: Source parameterization and ground motion levels, Bull. Seism. Soc. Am., 1998, 88: 881—897.
3. Zhao, Z. X., Xu, J. R., Horiuchi, H., Differentiation operation in the wave equation for the pseudospectral method with a staggered mesh, Earth Planets Space, 2001, 53: 327—332.
4. Somerville, P. G., Smith, N. F., Graves, R. W., Modification of empirical strong ground motion attenuation relations to include the amplitude and duration effects of rupture directivity, Seismological

Research Litters, 1997, 68: 199—222.
5. Iwata, T., Hatayama, K., Kawase, H. et al., Site amplification of ground motions during aftershocks of the 1995 Hyogo-ken Nanbu earthquake in severely damaged zone——Array observation of ground motions in Higashinada ward, Kobe city, Japan, J. Phys. Earth., 1996, 44: 553—561.
6. Zhao, Z. X., Kubota, R., Suzuki, F. et al., Crustal structure in the Southern Kanto-Tokai region derived from tomographic method for seismic explosion survey, Journal of Physics of the Earth, 1997, 45: 433—453.
7. Holzer, T. L., Youd, T. L. Hanks, T. C., Dynamics of liquefication during 1987 Superstition Hills, California earthquake, Science, 1989, 244: 56—59.
8. Kawase, H., The cause of the damage belt in Kobe: "The basin-edge effect," Constructive interference of the direct S-wave with the basin-induced diffracted/Rayleigh waves, Seismological Research Letters, 1996, 67: 25—34.
9. Zhao, Z. X., Xu, J. R., Staggered grid real value FFT differentiation and the application, Chinese Journal of Geophysics (in Chinese with English abstract), 2003, 46: 234—240.
10. Irikura, K., Causative fault, strong ground motion and damages from the 1995 hyogoken Nanbu earthquake, Butsuri-Tansa (in Japanese with English abstract), 1995, 48: 463—489.
11. Fukushima, Y., Tanaka, T., A new attenuation relation for peak horizontal acceleration of strong earthquake ground motion in Japan, Bull. Seism. Soc. Am., 1990, 80: 757—783.
12. Fujiwara, H., Takenaka, H., Calculation of surface waves for a thin basin structure using a direct boundary element method with normal modes, Geophys. J. Int., 1994, 117: 69—91.
13. Hao, X., Seo, K., Samano, T., Low damage anomaly of the 1976 Tangshan earthquake: An analysis based on the explosion ground motions, Bull. Seism. Soc. Am., 1994, 84: 1081—1027.
14. Kosloff, D., Reshef, M., Loewenthal, D., Elastic wave calculations by the Fourier method, Bulletin of the Seismological Society of America, 1984, 74: 875—891.
15. Yoshikawa, S., Ito, H., Summary for the 1995 Hyogo-ken Nanbu earthquake, Chikyu Monthly, Special issue (in Japanese), 1995, 13: 30—38.
16. Sekiguchi, H., Irikura, K., Iwata, T. et al., Minute locating of faulting beneath Kobe and the waveform inversion of the source process during the 1995 Hyogo-ken Nanbu, Japan, earthquake using strong ground motion records, J. Phys. Earth., 1996, 44: 473—487.
17. Pitraka, A., Irikura, K., Iwata, T., Three-dimensional simulation of the near-fault ground motion for the 1995 Hyogo-ken Nanbu (Kobe), Japan, earthquake, Bull. Seism. Soc. Am., 1998, 88: 428—440.
18. Kawase, H., Matsushima, S., Graves, R. W. et al., Three-dimensional wave propagation——The cause of the damage belt during the 1995 Hyogo-ken Nanbu earthquake, Zishin (in Japanese with English abstract), 1998, 50: 431—449.
19. Zhao, Z. X., Xu, J. R., Kubota, R. et al., Collapse ratios of buildings due to the 1995 Kobe earthquake and interference between S-wave and the second surface wave at basin edge, Chinese Science Bulletin, 2004, 49(2): 189—195.
20. Ishikawa, K., Mizoguchi, S., Oshika, A., Geology in Kobe area and investigation of the disaster on the 1995 south Hyogo great earthquake, Journal of the Japan Society of Engineering Geology (in Japanese with English abstract), 1995, 36: 62—80.
21. Aki, K., Local site effects on weak and strong ground motion, Tectonophysics, 1993, 218: 93—111.
22. Zhao, Z. X., Kubota, R., The distribution of strong ground motion from uppermost crustal structure——Comparison with disaster from the Hyogo-ken Nanbu earthquake, Proceeding of the 97th SEGJ Conference (in Japanese with English abstract), 1997, 71—74.
23. Zhao, Z. X., Xu, J. R., Horiuchi, S., Staggered grid real value FFT differentiation operator and its application for wave propagation simulation in heterogeneous medium, Chinese Journal of Geophysics, 2003, 46: 324—333.
24. Hu, L. X., Engineering Seismology, Beijing: Seismologic Press, 1988, 150—173.
25. Reshef, M., Kosloff, D., Edwards, M. et al., Three-dimensional elastic modeling by the Fourier method, Geophysics, 1988, 53: 1184—1193.
26. Furumura, T., Kennett, B. L. N., Takenaka, H., Parallel 3-D pseudospectral simulation of seismic wave propagation, Geophysics, 1998, 63: 279—288.
27. Wang, Y., Takenaka, H., Furumura, T., Modelling seismic wave propagation in a 2-D cylindrical whole earth model using the pseudospectral method, Geophys. J. Int., 2001, 145: 689—708.
28. Zhao, Z. X., Xu, J. R, Yang, W. C. et al., Simulations of reflection seismic profile of borehole area of Chinese Continental Scientific Drilling, Acta Petrologica Sinica (in Chinese with English abstract), 2004, 20: 127—136.
29. Zhao, Z. X., Xu, J. R., Basin geological structure and the simulations for mechanism of seismic disaster, Acta Geologica Sinica, 2004, 78: 954—959.
30. Kubo, T., Earthquake-resisting technologies for building structures, evaluation of seismic resisting capacity of existing buildings brick-wall buildings in Shanghai, China, in WG-1 Earthquake-resisting Technologies for Building Structures, 3rd EQTAP Workshop, Nov 28—30, 2000, Manila Philippines. Organization Committee for the 3rd EQTAP Workshop, 2000, 67—74.
31. Cerjan, C., Kosloff, D., Koskoff, R. et al., A nonreflecting boundary condition for discrete acoustic and elastic wave equations, Geophysics, 1985, 50: 705—708.
32. Furumura, T., Takenaka, H., A stable method for numerical differentiation of data with discontinuities at end-points by means of Fourier transform-symmetric differentiation, Geophys. Expl., 1992, 45: 303—309.
33. Boatwright, K., Correlation of ground motion and the intensity for the 17 January 1994 Northridge, California Earthquake, BSSA, 2001, 91: 739—752.

(Received April 5, 2004; accepted June 15, 2004)